Computational Materials Science xxx (2017) xxx-xxx

Contents lists available at ScienceDirect

Computational Materials Science

journal homepage: www.elsevier.com

Effects of external electric field on the optical and electronic properties of blue phosphorene nanoribbons: A DFT study

D.A. Ospina[a], C.A. Duque[a], M.E. Mora-Ramos[b], J.D. Correa[c,*]

[a] Grupo de Materia Condensada-UdeA, Instituto de Física, Facultad de Ciencias Exactas y Naturales, Universidad de Antioquia UdeA, Calle 70 No. 52-21, Medellín, Colombia
[b] Centro de Investigación en Ciencias-IICBA, Universidad Autónoma del Estado de Morelos, Av. Universidad 1001, CP 62209 Cuernavaca, Morelos, Mexico
[c] Departamento de Ciencias Básicas, Universidad de Medellín, Medellín, Colombia

ARTICLE INFO

Article history:
Received 6 January 2017
Received in revised form 25 March 2017
Accepted 30 March 2017
Available online xxx

Keywords:
Phosphorene
Optical
DFT
Nanoribbons

ABSTRACT

Using first principles calculations we investigate the effect of external electric fields in the optical and electronic properties of blue-phosphorene nanoribbons. It is shown that the application of a static external electric field serves as a tool for controlling the band gap of blue-phosphorene nanoribbons. Accordingly, the system will show a transition from semiconductor to metal, depending on the intensity of the applied electric field and the width of the nanoribbon. Our results for the imaginary part of the dielectric function suggest that the optical properties of the blue-phosphorene nanoribbons can be modulated through of the electric field as well.

1. Introduction

In recent years the investigation of phosphorus-based structures has emerged through the possibility of obtaining two-dimensional (2D) monolayer systems from black-phosphorus [1]. The crystal structure of black-phosphorus is consists of a stacking of quasi-planar corrugated layers. These layers interact by means of van der Waals forces in a way similar to graphite. As a consequence, using mechanical exfoliation it becomes possible to produce an atomic black-phosphorus monolayer system which has been named as phosphorene [2]. The phosphorene, both in the pristine and functionalized forms [3], has shown novel physical, chemical, and mechanical properties, that can be used to design and fabricate new optical and electronic devices [4], such as field effect transistors [5].

Due to these features, other 2D phosphorus allotropes have been explored [3,6–9]. Among the distinct allotropic forms, the so-called blue-phosphorene (BP) exhibits a fairly good thermodynamical stability as a black-phosphorus monolayer structure [6,10]. The 2D BP is a quasi-planar isotropic hexagonal layer of phosphorus atoms that can be obtained by means of a specific dislocation of the phosphorene array of atoms [6]. It is a semiconductor with indirect fundamental energy band gap. The B-substituted BP turns out to be direct band gap semiconductor, whereas C- and O- substituted BP shows magnetic properties [11]. Very recent reports indicate that hydrogenated and halogenated BP is a Dirac material [12].

Unlike graphene, the 2D monolayers of phosphorus atoms exhibit an energy band gap (EBG) in their electronic structures. The value measured by photoluminescence spectra of the EBG of phosphorene onto Si/SiO substrate is 1.45 eV [4]. Theoretical calculations using density functional theory (DFT), without many-body corrections, predict a value of the EBG of 0.8 eV for free-standing phosphorene, and when the many-body corrections are included the valued obtained is 1.4 eV [13]. In the case of BP, theoretical calculations have predicted an EBG of 2 eV [6].

One of the important characteristics of the EBG of 2D nanostructures is that it is possible to modulate it either by changing the geometry of by employing external probes such as electromagnetic fields. For example, in phosphorene the band gap is tuned via the number of stacked layers. As long as the number of layers increases the EBG will decrease [1].

Another possibility to modulate the band gap is the cutting of the 2D phosphorus monolayer in the form of finite-width size nanoribbons [14–17]. In these nanoribbons, the physical properties become further modified by the confinement of the electron motion along one particular direction [14]. Analogous to the case of graphene nanoribbons, phosphorene nanoribbons (PNRs) can have different edges; a fact that changes their physical properties. For instance, the zigzag-oriented phosphorene nanoribbons (zPNRs) with unpassivated edges are metals, whereas the unpassivated-edges armchair phosphorene nanoribbons (aPNRs) are semiconductors [14]. In the case of edge passivation, the dependence of the EBG of PNRs with the nanoribbon width (w), is of the form $1/w$ for zigzag edge, and $1/w^2$ for armchair edge [15]. In addition, the EBG of PNRs can be tuned by varying the width of the ribbon, as shown by Xie et al. in Ref. [16]. Dif-

* Corresponding author.
Email address: jcorrea@udem.edu.co (J.D. Correa)

http://dx.doi.org/10.1016/j.commatsci.2017.03.048
0927-0256/

ferently to the reports in [14,15], the work of Ref. [16] deals with the particular case of the BP allotrope, describing the features of the quantum confinement effect in zigzag and armchair BPNRs with hydrogen saturation on both sides. They found that both systems are indirect semiconductors with increasing EBG when the NR width are reduced. Carvalho et al. have studied the edge induced gap states using both analytical models and DFT [18].

It is possible to mention an additional number of previous works on PNRs. Using first-principles calculations, different properties of black phosphorene NRs are reported. For instance, Zhu et al. [19] studied the electronic and magnetic properties of zigzag black PNRs. They obtained that hydrogen-passivated structures are non-magnetic direct gap semiconductors and oxygen-passivated NRs show magnetic ground state. Zhang and collaborators [20] used DFT to investigate the electronic properties of armchair and zigzag black PNRs. Without edge passivation, their armchair NRs are semiconducting – with the gap being decreased as long as the ribbon's width augments, whilst the zigzag NRs are metallic. Under edge passivation, both kinds of NRs exhibit semiconductor behavior. In Ref. [21], the authors considered passivated strained NRs. Their results show a significant quantum size effect and a quite important effect of strain on the electron and hole effective masses. In addition, DFT studies on edge-passivation (using hydrogen and fluorine) effect on the band gap and effective mass of electrons in zigzag black PNRs show a band gap opening of up to 2.25 eV [22]. The influence on uniaxial stress in these nanostructures was reported by Sorkin and Zhang [23]. Scaling laws of band gaps in PNRs were studied in Ref. [24] using tight-binding techniques. Along these lines, they find that for armchair PNRs, an insulator-metal transition can be expected when a transverse electric field is applied. Furthermore, Du et al. have discovered the unexpected magnetic semiconductor behavior of zigzag black PNRs driven by half-filled one-dimensional band [25], whilst Yu and collaborators have used DFT and non-equilibrium Green's functions to investigate the electronic and transport properties of black phosphorene armchair and zigzag NRs under an external transverse electric field, reporting the presence of a giant Stark effect [26].

More recently, the properties of black-phosphorene based NRs were investigated by Páez et al., taking into account the presence of constriction on one of the edges. First principles calculations by Zhang and collaborators revealed the effect of strain and different passivation groups on black PNRs [27]. Nourbakhsh and Asgari used the GW method and the Bethe-Salpeter equation to study the optical and excitonic properties [28]. The room-temperature magnetism on the zigzag edges of black phosphorene nanoribbons was reported in Ref. [29]. First-principles quantum transport calculations were used to investigate the effects of the edge types and edge defects on the electronic and transport properties of that kind of PNRs [30]. Finally, the work by Fan et al. deals with the transport properties of Schottky contact structure based on zigzag PNR by using the non-equilibrium Green's function formalism and the density functional theory [31].

The case of blue PNRs has been less present in the literature. We find, for instance, the work by Xie and collaborators [16], based on first principles calculations. They discuss a quantum confinement mechanism for the band gaps of armchair and zigzag BPNRs as a function of their widths. The carrier mobilities in the same kind of structures were the subject of the article [32]. There, the authors used DFT and Boltzmann transport theory within the relaxation time approximation, and found that armchair and zigzag BPNRs are p-type semiconductors provided hole mobilities are one order of magnitude larger than electronic ones. The electronic structure and magnetism of zigzag BPNRs, including passivation effects were the subject of the study in [33], with focus on the variation of the nanoribbon widths. The possibility of using ultra-narrow BPNRs for tunable optoelectronics is discussed by Swaroop et al. [34], who report on the optoelectronic properties of such structures within the state-of-the- art density functional theory framework.

All of the above mentioned features turn 2D phosphorene allotropes into potential candidates to develop a number of electric applications like thin-film solar cell, field effect transistors, gas sensors, and lithium-ion batteries [4,35,36,5,37]. On the other hand, due to the importance of a better knowledge of the optical properties of the 2D phosphorus allotropes – and their possible use in new optoelectronic devices, several studies have been reported [38,39,15,13]. In the case of black-phosphorene monolayers, time-dependent density functional theoretical (TDDFT) calculations of the optical response have shown a large absorption in the ultraviolet region and proved that the inclusion of edge effects greatly affects the absorption spectrum of phosphorene [39]. The effect of edges has also been investigated for black-phosphorene nanoribbons via first principles calculations, showing a strong dependence of the optical spectrum on the features of the edged geometry of nanoribbons [15]. Actually, in the case of few-layer black phosphorous, theoretical calculations including many-body effects showed that the optical absorption is only possible for light polarized along the armchair direction [15].

Motivated by the possibilities opened by the use of the phosphorus-allotrope 2D nanostructures, and the comparatively lesser presence of the BPNRs in the literature on the subject, in this work we shall study the optical and electronic properties of the BPNRs under the influence of externally applied electric fields. Our aim is to investigate the combined effects of charge carrier confinement along one dimension and the electric field on the basic physical properties of these particular nanosystems. For that purpose we perform DFT calculations as detailed in the next section. It includes the theoretical framework of the study, whilst the Section 3 and 4 are respectively dedicated to present and discuss the obtained results and to give the conclusions of the work.

2. A brief on the theoretical approach

Our DFT calculations were carried out by using the SIESTA *ab initio* package [40], which employs norm-conserving pseudopotentials together with localized atomic orbitals as a basis set (double-ζ, single polarized, in the present work). For the exchange-correlation functional we consider the generalized gradient approximation (GGA) of Perdew-Burke-Ernzerhof [41].

The BPNRs are studied within the supercell approach with periodic boundary conditions along the nanoribbon-growth direction [x for armchair (aBPNRs) and y for zigzag (zBPNRs) geometries]. The BPNRs were fully relaxed by the conjugate gradient minimization until the forces on the atoms were less than 0.02 eV/Å. The schematic view of the equilibrium geometric setup obtained after relaxing the BPNRs, is depicted in Fig. 1. Fig. 1(a) shows a zigzag edged BPNR, whilst Fig. 1(b) shows the armchair edged BPNR. As can be noticed, the edges are assumed to be passivated, in this case with hydrogen atoms.

The Brillouin zone is sampled using a Monkhorst-Pack mesh of $9 \times 1 \times 1$ for aBPNRs and $1 \times 9 \times 1$ for zBPNRs. These grids ensure the total energy convergence. In addition, the optical absorption spectrum is obtained in the framework of the independent particle approximation, through the imaginary part of the dielectric function; which

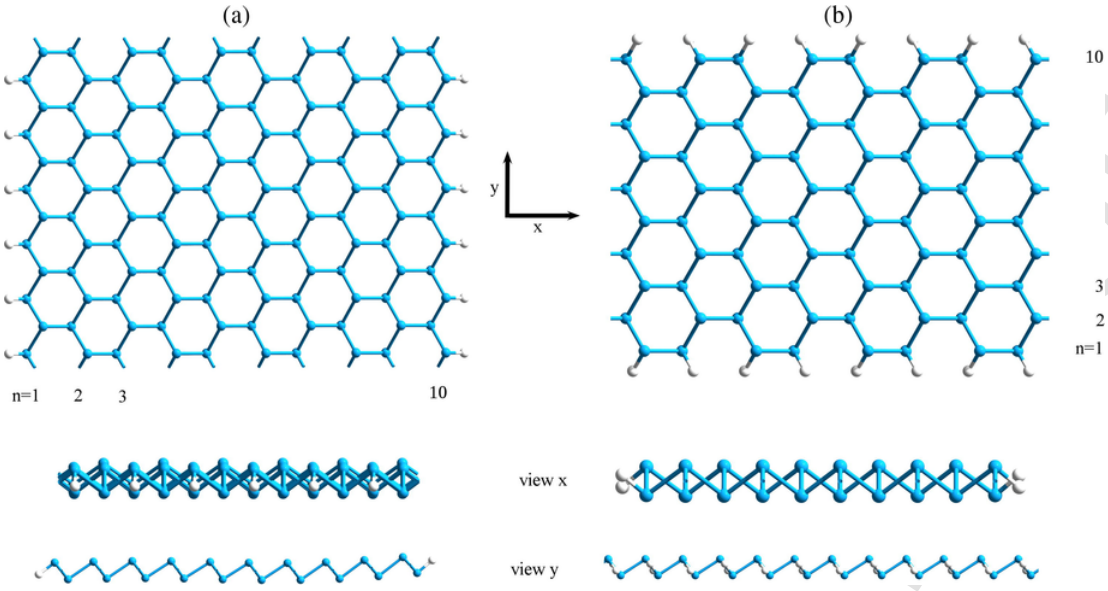

Fig. 1. Schematic representation of blue phosphorene nanoribbons. Two different edge configuration are shown: (a) zig-zag and (b) armchair. Distinct views of the structures are also shown.

is given by:

$$\varepsilon_2(\omega) = A \int d\mathbf{k} \sum_{c,v} |\hat{\epsilon} \cdot \langle \Psi_c(\mathbf{k}) | \vec{r} | \Psi_v(\mathbf{k}) \rangle|^2 \delta(E_c(\mathbf{k}) - E_v(\mathbf{k}) - \hbar$$

In this expression, A is a cell-volume-dependent constant, while $\Psi_{c,v}$ are occupied an unoccupied Kohn-Sham states. Energy conservation is guaranteed with the delta function but, in practice, it is replaced by a Gaussian function with HWHM equal to 0.06 eV. Two polarizations of the incident light are considered: x and y directions as indicated in Fig. 1. In order to ensure the convergence of the optical absorption spectrum we have used a k-grid points of $100 \times 1 \times 1$ and $1 \times 100 \times 1$. These k-grids also were employed to calculate the total density of states (DOS).

The independent particle approximation does not take into account the many-body effect as it is done by the GW corrections or by the inclusion of electron-hole interaction – which are needed to provide an accurate description of the optical spectrum. However, due to the difficulty of incorporating the many-body effect in the case of large systems, the independent particle approximation is extensively applied, looking for an understanding of the basic properties of the optical spectrum as the selection rules, geometric effects as well as external field effects [15,42].

3. Results and discussion

In this work we study BPNRs of different widths. In order to specify the width of a nanoribbon we make use of the standard notation n-aBPNR and n-zBPNR [14]. Here, n represents the number or zigzag lines for zBPNRs, and the number of dimer lines for aBPNR as it is shown in Fig. 1.

The calculated lattice constants are 3.32 Å for zBPRNs and 5.76 Å for aBPNRs. The distance between phosphorus atoms is 2.29 Å in both cases. These results are in agreement with a previous theoretical report [14].

The zero field energy band structures for aBPNRs and zBPNRs are shown in Fig. 2. Several ribbon widths are considered. Fig. 2(a)–(c) are for 6-aBPNR, 10-aBPNR and 14-aBPNR, respectively. It can be noticed that in all cases, aBPNRs are semiconducting systems, with the main energy gap having an increase as long as the width of the ribbon is reduced (reaching almost 3 eV in the $n = 6$ case). As can be noticed, the fall in the value of the gap with augmenting n results from a shift upwards of the whole spectrum – using the Fermi energy as a zero reference, with the largest displacement for the valence band energies; although the overall shift becomes diminished as n augments.

On the other hand, the qualitative features of the spectrum are kept when the number of dimer lines augments, being the more notorious of them the quasi-flatness of the top valence band. The confinement of the carrier motion along the transverse nanoribbon direction causes the additional quantization of the spectrum, leading to the appearance of what is known in the physics of low-dimensional systems as energy subbands. Therefore, one may notice the presence of a greater number of dispersion curves within a given energy interval, in comparison with the typical spectrum of a 2D phosphorene monolayer [16].

With regard to the zBPNRs, the zero field energy spectrum also reveals the semiconducting character of the structure. Fig. 2(d)–(f) are for 4-zaBPNR, 8-zBPNR, and 10-zBPNR, respectively. In this case, the value of the main EBG is less sensitive to the increment of the number of zigzag lines, showing only a little decrement for the values of n considered. It can be noticed the rise in the number of allowed states within the same energy intervals. This is also a consequence of the increase in the ribbon width, as the carrier localization becomes smaller. Nonetheless, the main qualitative features of the spectrum – mainly in the case of the upper valence and lower conduction bands – remain unchanged.

Our results for zero electric field agree well with those previously reported [16,33]. In particular, the shape of the band structure for hydrogen-passivated aBPNRs and zBPNRs is reproduced, including the quasi-flatness of the top valence band that has been previously observed. Furthermore, in order to compare our results for zero applied electric field with the previous report of Ref. [16], in Fig. 3 we show

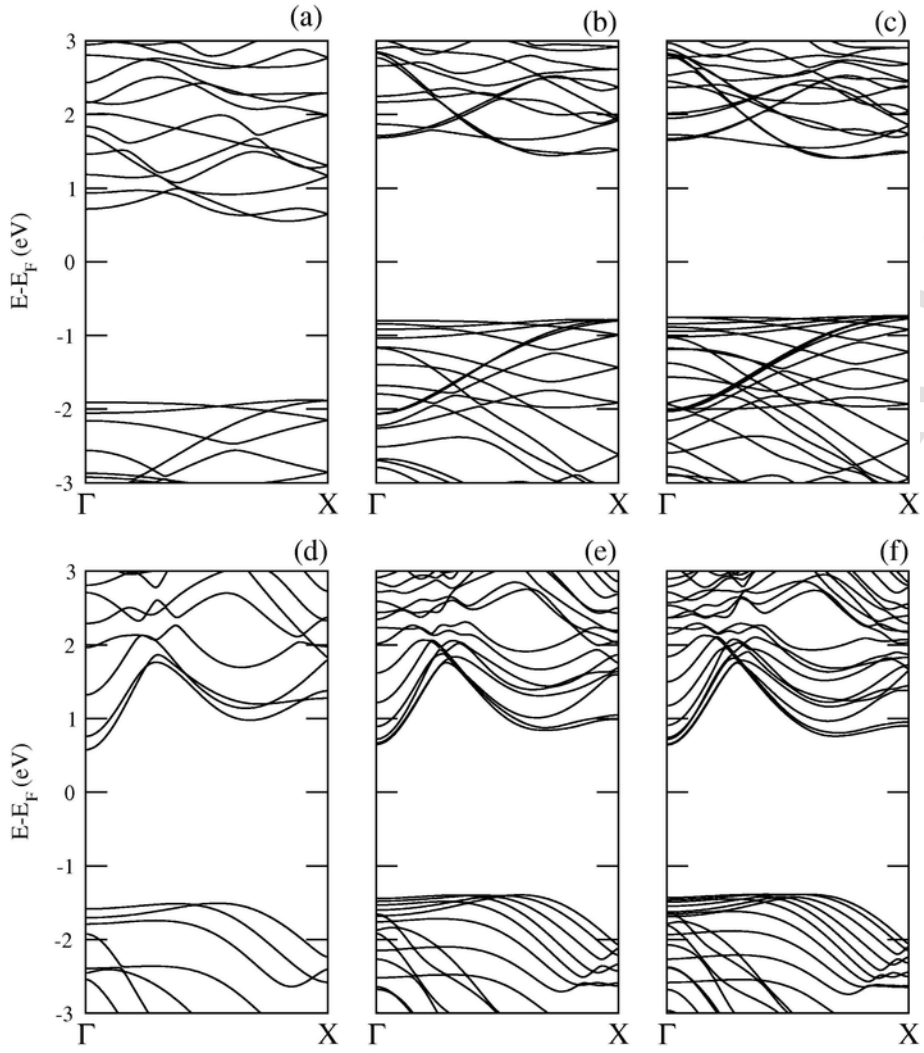

Fig. 2. DFT band structure of armchair and zig-zag blue phosphorene nanoribbons. Three representative widths are considered in each case: (a) 6-aBPNR, (b) 10-aBPNR, (c) 14-aBPNR, (d) 4-zBPNR, (e) 8-zBPNR and (f) 10-zBPNR.

the variation 0f the EBG for aBPNR and zBPNR as a function of the nanoribbon width. The solid line represents the result of fitting the band gap by $E_{gap} = E_0 + \gamma w^{-1}$, where $E_0 = 2$ eV is the EBG of blue phosphorene monolayer and γ is a fitting parameter of value 3.936 ± 0.18 eV Å for aBPNRs and 1.38 ± 0.16 eV Å for zBPNRs, as is reported in Ref. [16]. It can be noticed that the values obtained by us follow the same trend there reported. Consequently, it can be said that the calculation performed in this work – for zero electric field – reproduces previous findings on the subject.

Figs. 4(a)–(c) and 5(a)–(c) contain our results for the calculated total DOS in the armchair and zigzag nanoribbon cases, respectively. The comments made above with regard to the features of the energy band structure are confirmed by observing these figures.

In addition, in Figs. 4(d), (e) and 5(d), (e) we are presenting the calculated imaginary part of the dielectric function for the armchair and zigzag BPNRs under consideration. As it is known, this quantity actually represents the interband optical absorption response of each structure. Two distinct polarizations of the incident light are considered in each case, leading to significant changes in the optical absorption spectrum of the BPNRs, mainly for the armchair geometry. This indicates a change both in the selection rules that govern the realization of a particular valence to conduction band transition and in the value of the corresponding electric dipole moment expected value. For the sake of comparison, the light absorption spectrum of a single monolayer BP is shown in the insets. It is noticed that when the incident light is polarized parallel to the aBPNR growth-direction or perpendicular to the zBPNR, the calculated optical response resembles more closely that of the BP monolayer, with a clear tendency of a better approaching when the number of atomic lines is larger, as expected. Even so, one may notice that the main absorption peaks in the cases of BPNRs are blueshifted with respect to the corresponding one in the BP monolayer.

Another interesting feature regarding the main light absorption peak in BPNRs is the fact that it appears located somewhat above the energy value of 4 eV. Keeping in mind that the present calculation is performed at $T = 0$ K, this indicates that the associated valence to conduction band transition most probably takes place between the top of the valence band and an energy subband located approximately 2 eV above of the conduction band bottom.

Changing the subject, the influence of the application of a static electric field oriented perpendicularly to the nanoribbon growth-direction onto the EBG of aBPNRs and zBPNRs is presented in

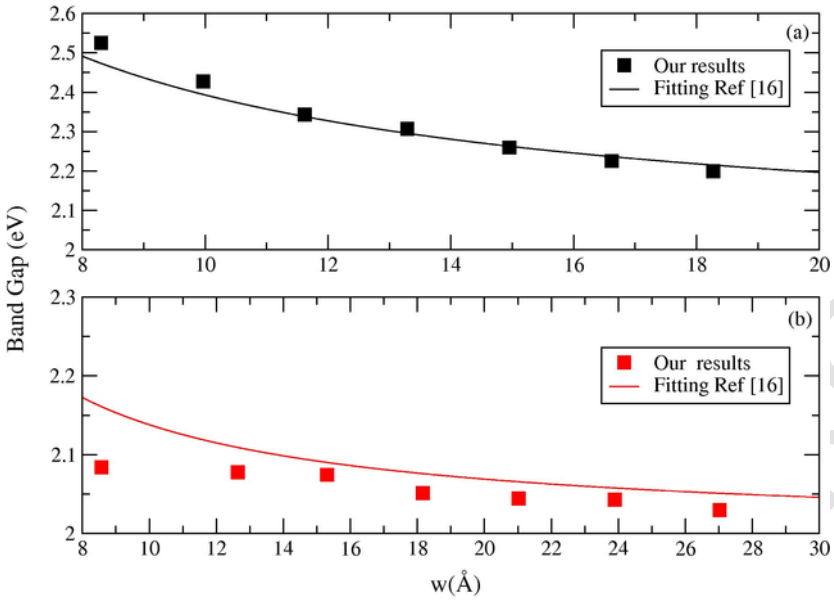

Fig. 3. Band gap as a function of the width (w) of blue phosphorene nanoribbons. (a) aBPNR and (b) zBPNR. Square points represent our result and solid line represent the fitting equation in the Ref. [16].

Fig. 6(a) and (b), respectively. It can be readily noticed that the progressive increment of the electric field intensity causes a significant reduction of the EBG in these structures. The rate of decreasing of this quantity as a function of the field strength is modulated by the number of armchair dimers or zigzag lines that determine the width of the nanoribbons. For narrower ribbons, the reduction of the EBG occurs at slower pace whereas for wider ribbons, the fall takes place more rapidly. This process may lead to the metallization of the system by making the EBG to become zero for strong enough electric fields. The wider the ribbon, the smaller the value of field intensity needed to induce the insulator-metal transition. Moreover, the described effect is more pronounced for zBPNRs. As can be seen from Fig. 6(b), for a 10-zBPNR, the zero EBG condition is reached for a relatively low value of the applied electric field.

For a better viewing of this phenomenon we have plotted the first principles calculated energy band structure of aBPNRs and zBPNRs under applied electric field in Figs. 7 and 8, respectively. For both geometrical setups, a narrow (upper panel) and a wide (lower panel) ribbon cases are reported for four different values of the electric field intensity including the zero field case. The evolution of the energy spectrum can be clearly observed, with a well defined transition to a metallic regime for high enough field intensity.

It is worth noticing the influence of the geometry in this phenomenon. For instance, in the zigzag case the qualitative picture of the spectrum is kept all along the interval of variation of the electric field, and the progressive reduction of the EBG is readily noticed. In the armchair case, the field effect causes a rather strong modification of the shape of the electronic structure, mainly for its valence band part.

We can resort to a simple argument to explain the properties shown by the spectrum of allowed energy values in these BPNRs. First of all, one may consider that the presence of hydrogen-passivated edges turns the confined motion of electrons along the nanoribbon growth direction as analogous to the problem of a carrier in a quantum well with infinitely high potential barriers. Then, the application of a static electric field along the same direction results in a lowering of the potential well bottom (for both conduction and valence band profiles). This leads to a shift of the conduction band states towards lower energies, and to a shift upwards of the valence band states. At a certain value of the field, such a relative displacement will induce the zero-gap condition in the structure. This process takes place with varying intensity for different directions within the Brillouin zone, depending on the strength of the applied field.

To illustrate the behavior of the band structure of the aBPNRs and zBPNR, in Fig. 9 we present the local density of states (LDOS) considering different values of the applied electric field, in two specific cases: 12-aBPNR and 10-ZBPNR. In particular, owing to understand the field-induced semiconductor-metal transition, we plot the LDOS associated to the valence band (VB) and conduction band (CV) states located nearest to the Fermi level.

In the case of the 12-aBPNR one may observe that at zero applied electric field the LDOS of VB and CB states in Fig. 9-a are spatially distributed over the entire structure and have different shapes. However, as long as the electric field intensity augments these LDOS tend to localize at the edges of the 12-aBPNR, whilst for the highest electric field values considered, the LDOS for VB and CB states become equal and are localized just at one of the nanoribbon edges. In the case of the 10-zBPNR, we observe the same kind of behavior. In accordance, it can be said that the transition semiconductor-metal in BPNRs – detected at sufficiently large electric field intensities – is caused by the localization of the states at the ribbon edges. This kind of redistribution that leads to the semiconductor-metal transition was previously report in the case of BN nanoribbons [43].

Another aspect to be pointed at, in this case, is the field-induced breaking of energy state degeneracies in what can be called as a quantum confined Stark effect. In this case, such a feature is better observed for wider nanoribbons, as expected.

The fact that the application of a static external electric field can result in a rather dramatic change of the energy spectrum – mainly in the EBG- may constitute a tool for modulating the electronic properties of this structures. In consequence, the possibility of their use in the design and fabrication of electronic devices becomes further enhanced.

Finally, the particularities of the valence band to conduction band optical absorption response of aBPNRS and zBPNRs appear depicted in Figs. 10 and 11, in which the calculated imaginary part of the di-

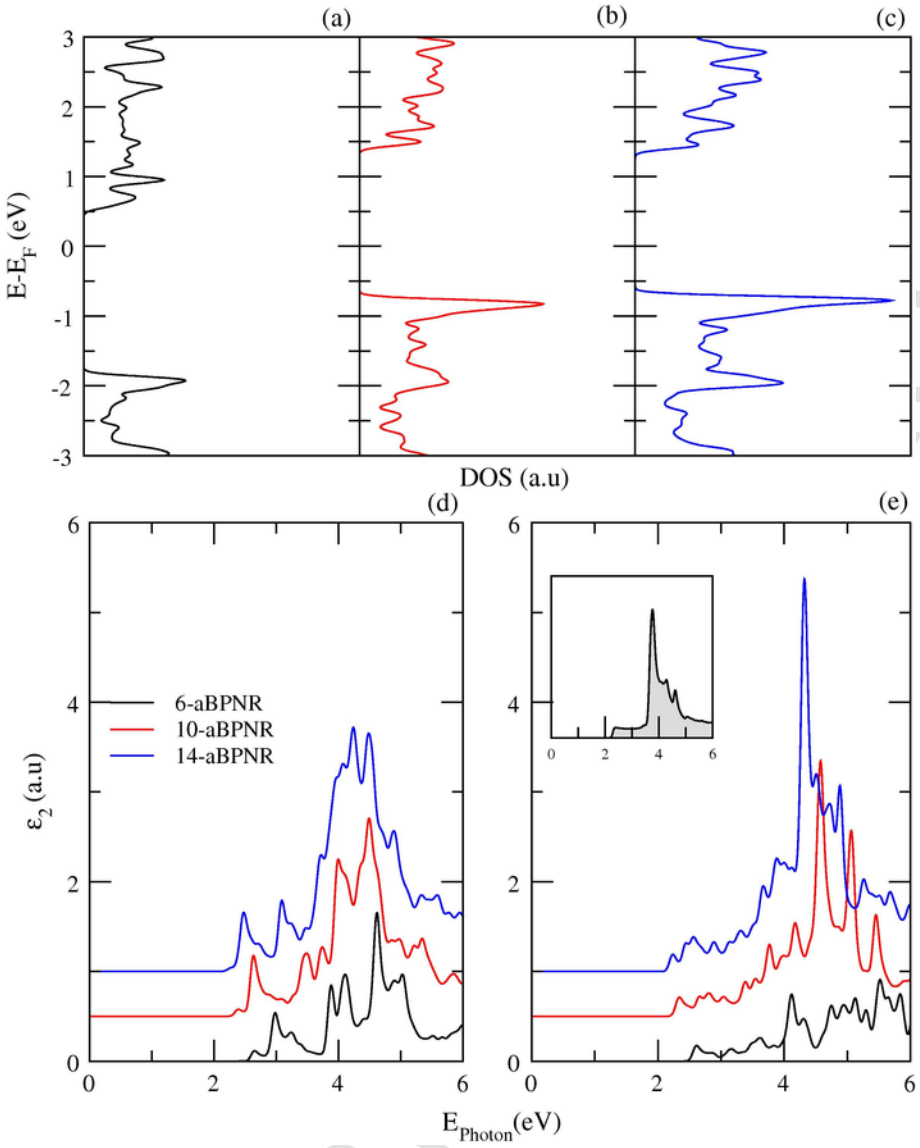

Fig. 4. Total density of states for armchair blue phosphorene nanoribbons. Three different ribbon widths are considered. (a) 6-aBPNR, (b) 10-aBPNR and (c) 14-aBPNR. In addition, the calculated imaginary part of the dielectric function of these three nanoribbons is shown as well, taking into account two polarizations of the incident light: (d) light polarized perpendicular, and (e) light polarized parallel to the armchair nanoribbon growth direction. The insert in the panel (e) contains the imaginary part of the dielectric function in the case of a blue phosphorene – extended – monolayer.

electric function is shown as a function of the incident photon energy for armchair and zigzag BPNRs respectively. Two different ribbon widths and two distinct polarizations of the incoming light have been taken into account.

In the armchair geometry, there is a relatively small influence of the electric field on the light absorption for both polarizations for the 6-aBPNR (Fig. 10(a) and (b)), with a redshift of the position of resonant peaks, together with an enhancement of some of their amplitudes, which are mainly noticed when the light polarization is such as the electric field lies perpendicular to the growth direction. However, there is a significant redshift as well as a reinforcement of some absorption peaks – compared with the zero field case – in the response of the 14-aBPNR (Fig. 10(c) and (d)), being more notorious when the light polarization is parallel to the growth direction.

The absorption response of the zBPNRs shows an analogous behavior, with a weaker redshift of the resonant signals for the narrower ribbon (4-zBPNR, Fig. 11(a) and (b)) and a larger displacement and amplitude enhancement when the nanoribbon has a greater width.

The above commented changes induced by the electric field on the electronic structure are responsible for the properties of the optical response of the BPNRs under study. It is worth noticing that there are interband transitions – mainly those related with larger energy differences – that are not much affected by those changes. In fact, depending on the particular light polarization, more significant field-induced variations has to do with the lower transition energies around the modified EBG value, for which new selection rules – associated among other things with the quantum confined Stark effect – appear.

At this point, it is worth to highlight the effect of the geometry in the optical properties of the systems investigated. This opens a possibility of the combined use of the edged setup, the electric field, and the size of the structures in order to design a particular optical response for practical applications.

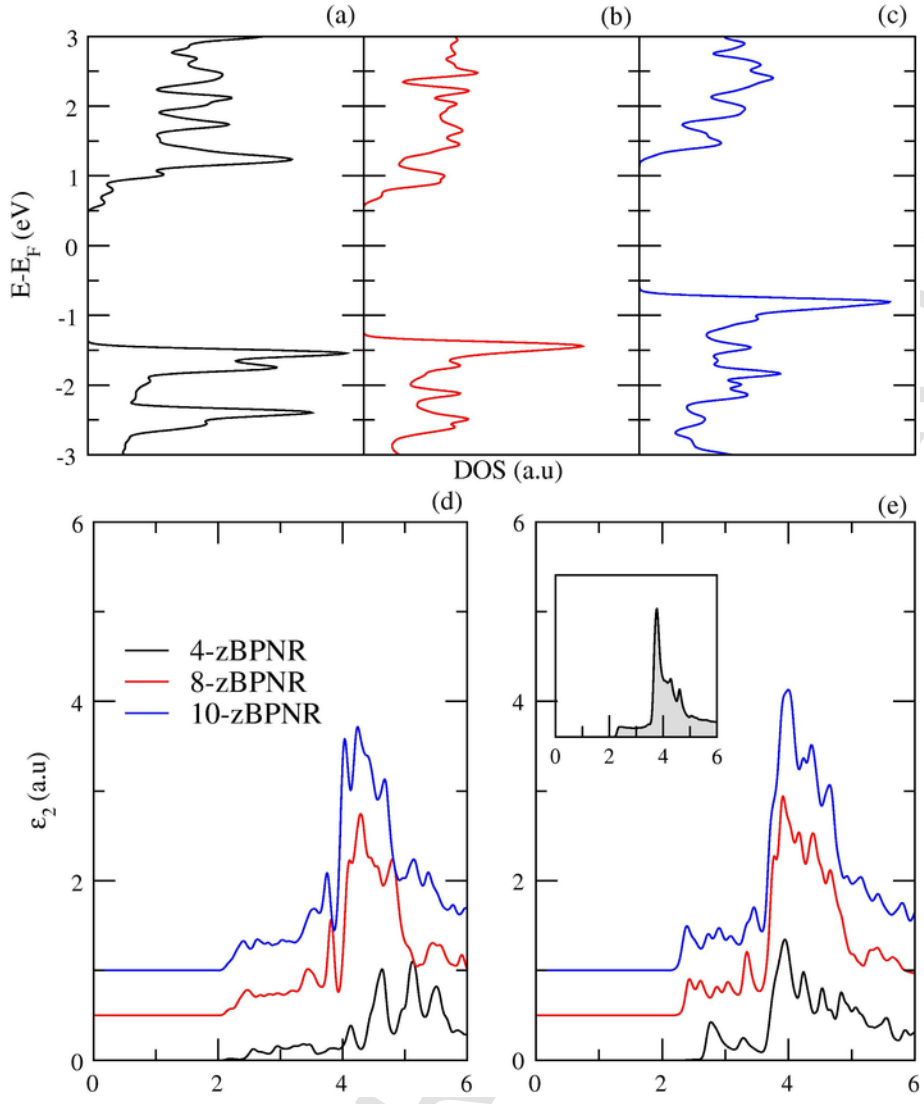

Fig. 5. Total density of states for zigzag blue phosphorene nanoribbon. Three different ribbon widths are considered: (a) 4-zBPNR, (b) 8-zBPNR and (c) 10-zBPNR. The imaginary part of the dielectric function of these three nanoribbons is shown in graphics (d) and (e). The calculation included two distinct polarizations of the incident photons: (d) light polarized parallel and (e) light polarized perpendicular to the zigzag nanoribbon growth direction. The insert in the panel (e) contains the imaginary part of the dielectric function in the case of a blue phosphorene – extended – monolayer.

4. Conclusions

In this work we have theoretically investigated the electronic and optical properties of blue phosphorene nanoribbons with and without the influence of external electric field. First principles density functional theory was used to perform the calculations. In particular we have explored the change of the electronic structure of the zig-zag and armchair blue phosphorene nanoribbons induced by a static electric field transverse to the nanoribbon grown-direction.

Our results show that in both kind of structures the energy band gap decreases as the electric field strength is augmented. Even for wide blue phosphorene nanoribbons and small field intensities it is detected a transition of the electronic spectrum from semiconducting to metallic character. This phenomenon could be employed to developed new tunable opto-electronic devices.

In addition, our theoretical results for the imaginary part of the dielectric function show that the interband linear optical response of the blue phosphorene nanoribbons is also affected by the changes in the electronic properties due to the influence of the applied electric field.

Acknowledgments

The authors acknowledge financial support from the Universidad de Medellín Research Office through Projects 746 and 747. DAO and CAD are grateful to the Colombian Agencies CODI-Universidad de Antioquia (Estrategia de Sostenibilidad de la Universidad de Antioquia and project: Manipulación de propiedades optoelectrónicas de nanoestructuras semiconductoras por ondas acústicas superficiales.), Facultad de Ciencias Exactas y Naturales-Universidad de Antioquia (CAD-exclusive dedication project 2015–2016), and El Patrimonio Autónomo Fondo Nacional de Financiamiento para la Ciencia, la Tecnología y la Innovación, Francisco José de Caldas. JDC thanks the colleagues at the CINC-UAEM, Cuernavaca, for hospitality during the preparation of this work.

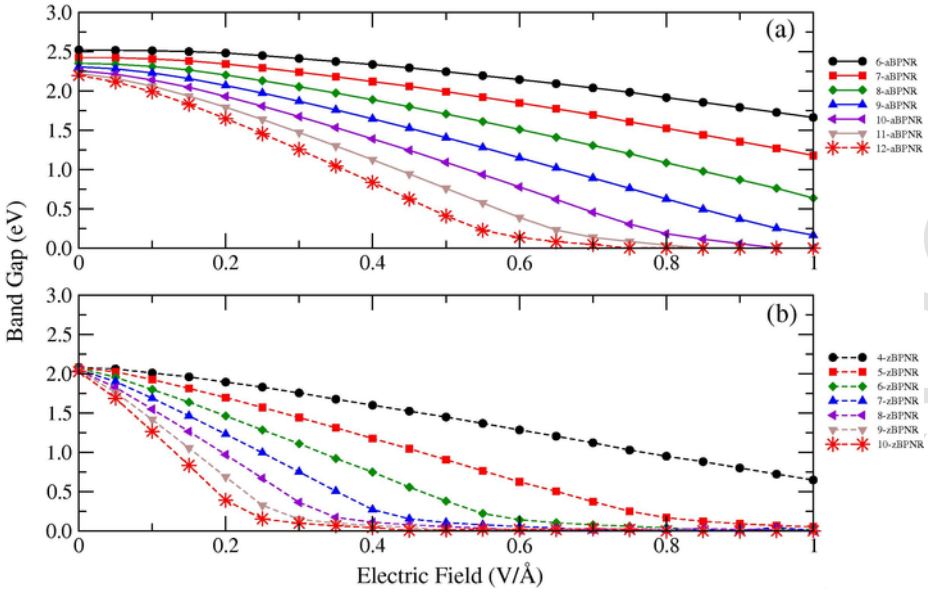

Fig. 6. The energy band gap as a function of the intensity of the externally applied electric field. Panel (a) is for the case of armchair blue phosphorene nanoribbons, and (b) for zigzag blue phosphorene nanoribbons. In both cases we have considered several values of the nanoribbon width.

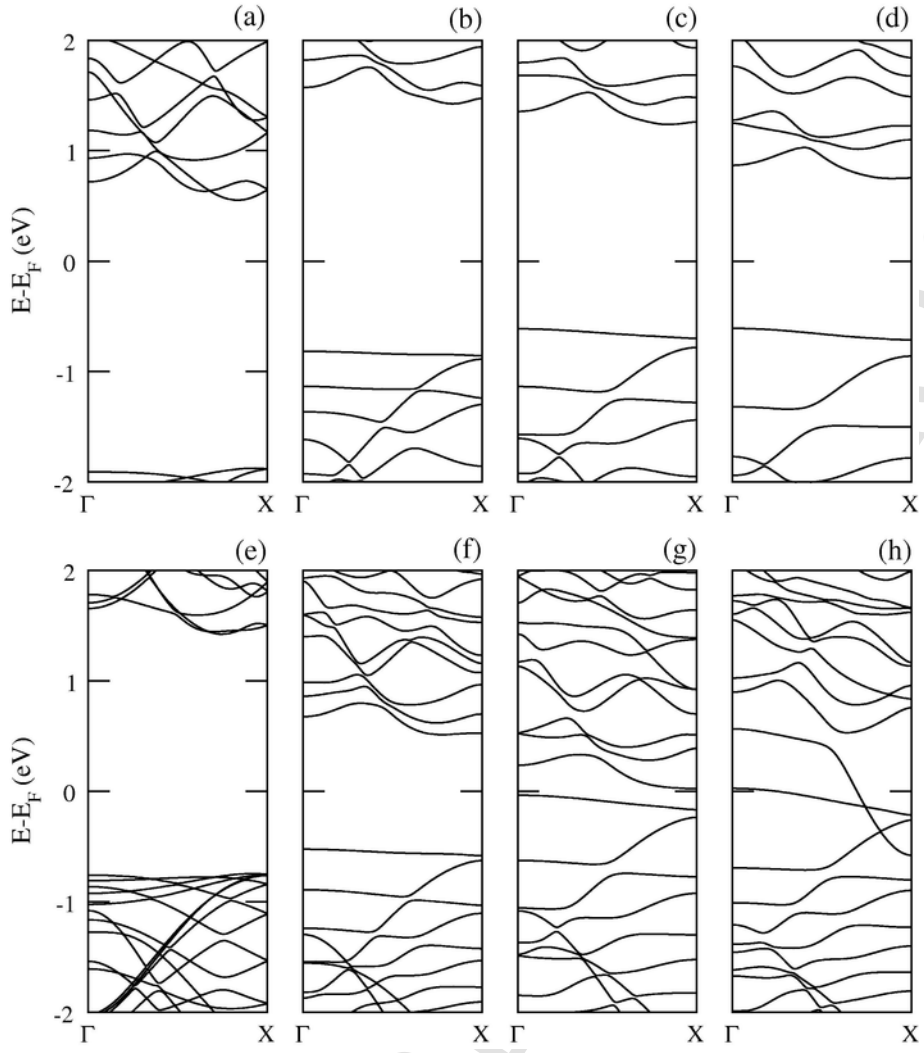

Fig. 7. Energy band structure of armchair blue phosphorene nanoribbons for different values of the electric field intensity: 0, 0.3, 0.6, and 0.9 V/Å. Two armchair nanoribbon widths are considered: 6-aBPNR (panels (a)–(d)), and 12-aBPNR (panels (e)–(h)).

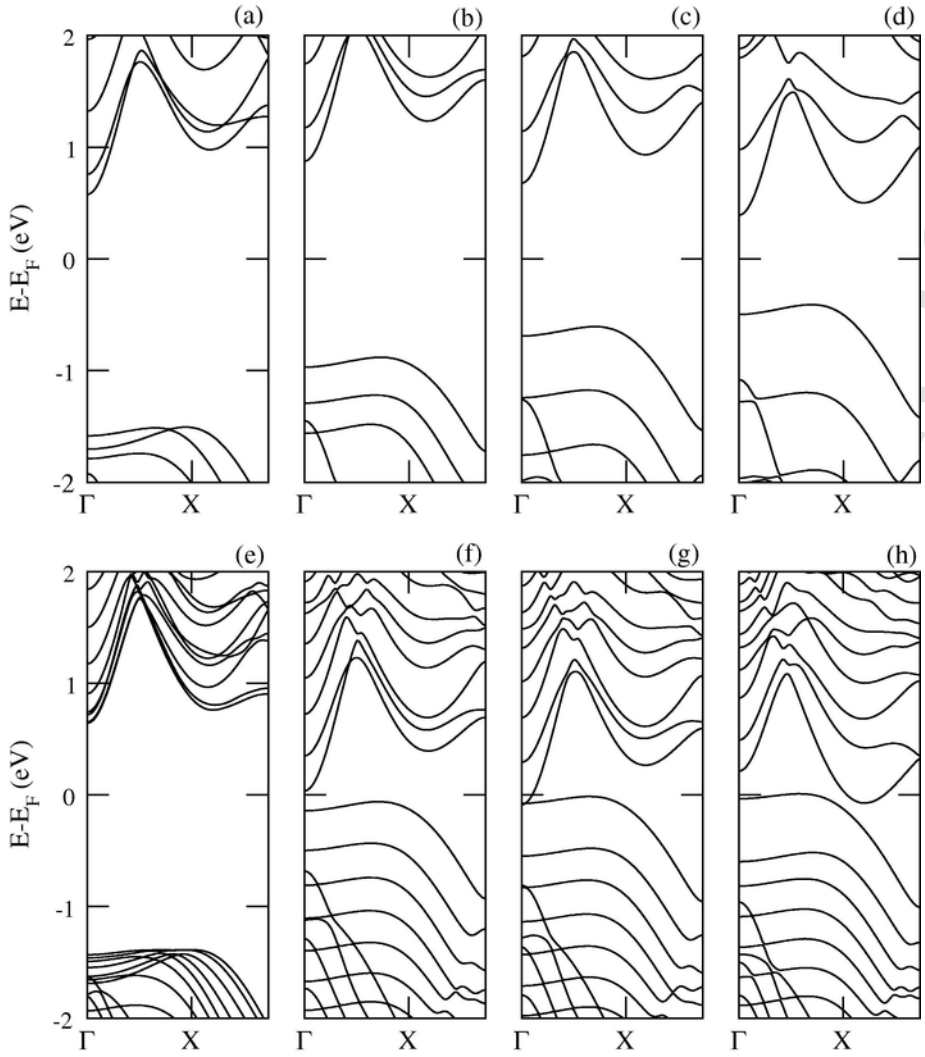

Fig. 8. Energy band structure of zigzag blue phosphorene nanoribbons for different values of the electric field intensity: 0, 0.3, 0.6, and 0.9 V/Å. Two zigzag nanoribbon widths are considered: 4-zBPNR (panels (a)–(d)), and 10-zBPNR (panels (e)–(h)).

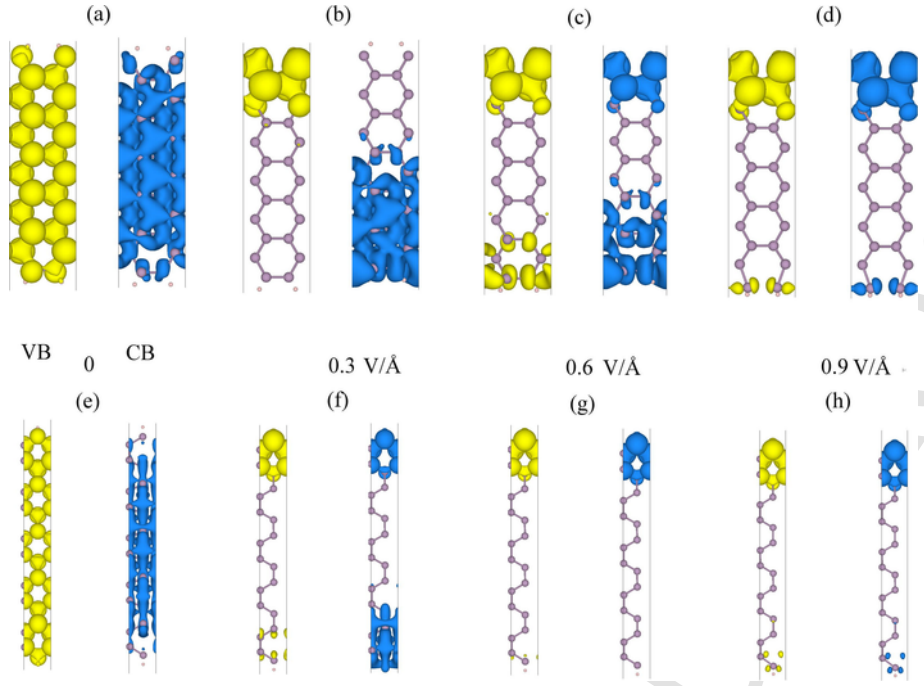

Fig. 9. Local density of states for 12-aBPNR (a–d) and 10-zBPNR (e–h), different values of the external electric field are considered. Yellow plot represent the valence state nearest to the Fermi level (VB) and blue surface plot represent the conduction state nearest to the Fermi level (CB). (For interpretation of the references to color in this figure legend, the reader is referred to the web version of this article.)

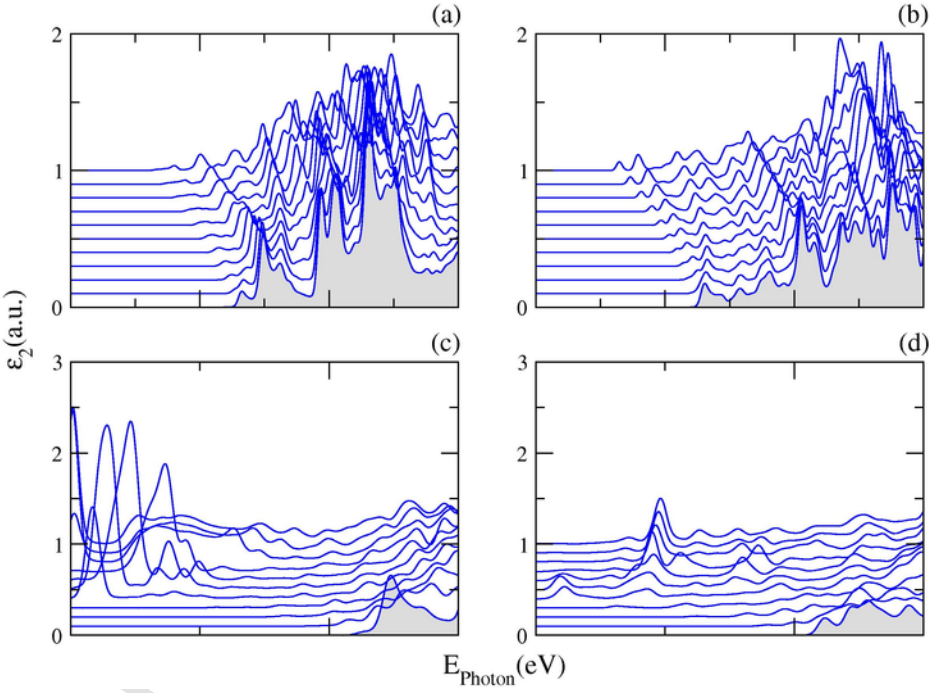

Fig. 10. Imaginary part of the dielectric function for armchair blue phosphorene nanoribbons of different widths. Panels (a) and (b) are for 6-aBPNR, (c) and (d) are for 14- aBPNR. Two polarizations of the incident light are considered: (a) and (c) correspond to light polarized parallel, and (b) and (d) correspond to light polarized perpendicular to the armchair nanoribbon growth direction. The absorption curves appear plotted for electric field intensities going from zero to 1 V/Å, with a step of 0.1 V/Å.

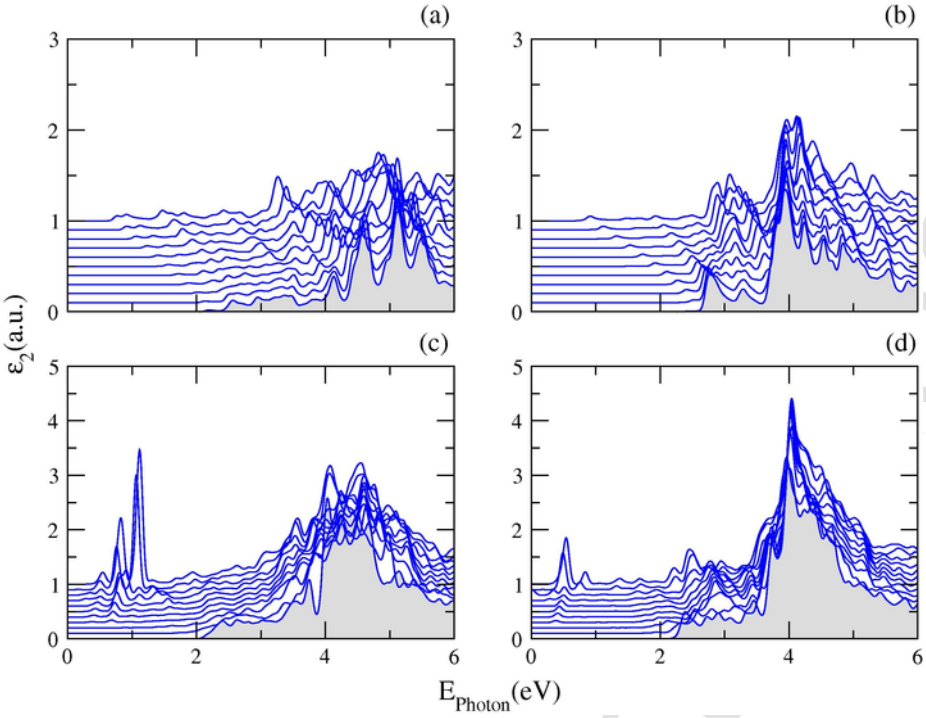

Fig. 11. Imaginary part of the dielectric function for armchair blue phosphorene nanoribbons of different ribbon widths. Panels (a) and (b) are for 4-zBPNR, (c) and (d) are for 10-zBPNR. Two polarizations of the incident light are considered, (a) and (c) light polarized perpendicular and (b) and (d) light polarized parallel to the zigzag nanoribbon growth direction. The absorption curves appear plotted for electric field intensities going from zero to 1 V/Å, with a step of 0.1 V/Å.

References

[1] X. Ling, H. Wang, S. Huang, F. Xia, M.S. Dresselhaus, The renaissance of black phosphorus, Proc. Natl. Acad. Sci. 112 (15) (2015) 201416581.

[2] H. Liu, A.T. Neal, Z. Zhu, Z. Luo, X. Xu, D. Tománek, P.D. Ye, Phosphorene: an unexplored 2D semiconductor with a high hole mobility, ACS Nano 8 (2014) 4033–4041.

[3] Y. Ding, Y.L. Wang, Structural, electronic, and magnetic properties of adatom adsorptions on black and blue phosphorene: a first-principles study, J. Phys. Chem. C 119 (2015) 10610–10622.

[4] L. Kou, C. Chen, S.C. Smith, Phosphorene: fabrication, properties, and applications, J. Phys. Chem. Lett. 6 (2015) 2794–2805.

[5] L. Li, Y. Yu, G.J. Ye, Q. Ge, X. Ou, H. Wu, D. Feng, X.H. Chen, Y. Zhang, Black phosphorus field-effect transistors, Nat. Nanotechnol. 9 (5) (2014) 372–377.

[6] Z. Zhu, D. Tománek, Semiconducting layered blue phosphorus: a computational study, Phys. Rev. Lett. 112 (2014) 176802.

[7] Y. Aierken, D. Çakr, C. Sevik, F.M. Peeters, Thermal properties of black and blue phosphorenes from a first-principles quasiharmonic approach, Phys. Rev. B 92 (8) (2015) 081408, http://dx.doi.org/10.1103/PhysRevB.92.081408.

[8] J. Guan, Z. Zhu, D. Tománek, Phase coexistence and metal-insulator transition in few-layer phosphorene: a computational study, Phys. Rev. Lett. 113 (4) (2014) 046804.

[9] J. Guan, Z. Zhu, D. Tománek, Tiling phosphorene, ACS Nano 8 (2014) 12763–12768.

[10] Y. Aierken, D. Çakr, C. Sevik, F.M. Peeters, Thermal properties of black and blue phosphorenes from a first-principles quasiharmonic approach, Phys. Rev. B 92 (8) (2015) 081408.

[11] M. Sun, W. Tang, Q. Ren, S.K. Wang, J. Yu, Y. Du, A first-principles study of light non-metallic atom substituted blue phosphorene, Appl. Surf. Sci. 356 (2015) 110–114.

[12] M. Sun, S. Wang, J. Yu, W. Tang, Hydrogenated and halogenated blue phosphorene as dirac materials: a first principles study, Appl. Surf. Sci. 392 (2017) http://dx.doi.org/10.1016/j.apsusc.2016.08.094.

[13] V. Tran, R. Soklaski, Y. Liang, L. Yang, Layer-controlled band gap and anisotropic excitons in few-layer black phosphorus, Phys. Rev. B 89 (23) (2014) 235319.

[14] H. Guo, N. Lu, J. Dai, X. Wu, X.C. Zeng, Phosphorene nanoribbons, phosphorus nanotubes, and van der Waals multilayers, J. Phys. Chem. C 118 (2014) 14051–14059.

[15] V. Tran, L. Yang, Scaling laws for the band gap and optical response of phosphorene nanoribbons, Phys. Rev. B 89 (2014) 245407.

[16] J. Xie, M.S. Si, D.Z. Yang, Z.Y. Zhang, D.S. Xue, A theoretical study of blue phosphorene nanoribbons based on first-principles calculations, J. Appl. Phys. 116 (7) (2014) http://dx.doi.org/10.1063/1.4893589.

[17] A. Ramasubramaniam, A.R. Muniz, Ab initio studies of thermodynamic and electronic properties of phosphorene nanoribbons, Phys. Rev. B 90 (8) (2014) 085424.

[18] A. Carvalho, A. Rodin, A.C. Neto, Phosphorene nanoribbons, EPL (Europhys. Lett.) 108 (4) (2014) 47005.

[19] Z. Zhu, C. Li, W. Yu, D. Chang, Q. Sun, Y. Jia, Magnetism of zigzag edge phosphorene nanoribbons, Appl. Phys. Lett. 105 (11) (2014).

[20] J. Zhang, H.J. Liu, L. Cheng, J. Wei, J.H. Liang, D.D. Fan, J. Shi, X.F. Tang, Q.J. Zhang, Phosphorene nanoribbon as a promising candidate for thermoelectric applications, Sci. Rep. 4 (2014) 4–10.

[21] X. Han, H. Morgan Stewart, S.A. Shevlin, C.R.A. Catlow, Z.X. Guo, Strain and orientation modulated bandgaps and effective masses of phosphorene nanoribbons, Nano Lett. 14 (8) (2014) 4607–4614.

[22] L.C. Xu, X.J. Song, Z. Yang, L. Cao, R.P. Liu, X.Y. Li, Phosphorene nanoribbons: passivation effect on bandgap and effective mass, Appl. Surf. Sci. 324 (2015) 640–644.

[23] V. Sorkin, Y.W. Zhang, The deformation and failure behaviour of phosphorene nanoribbons under uniaxial tensile strain, 2D Mater. 2 (3) (2015) 035007.

[24] E. Taghizadeh Sisakht, M.H. Zare, F. Fazileh, Scaling laws of band gaps of phosphorene nanoribbons: a tight-binding calculation, Phys. Rev. B 91 (2015) 085409.

[25] Y. Du, H. Liu, B. Xu, L. Sheng, J. Yin, C.-G. Duan, X. Wan, Unexpected magnetic semiconductor behavior in zigzag phosphorene nanoribbons driven by half-filled one dimensional band, Sci. Rep. 5 (2015) 8921.

[26] Q. Yu, L. Shen, M. Yang, Y. Cai, Z. Huang, Y.P. Feng, Electronic and transport properties of phosphorene nanoribbons, Phys. Rev. B 92 (3) (2015) 035436, http://dx.doi.org/10.1103/PhysRevB.92.035436.

[27] X. Zhang, Q. Li, B. Xu, J. Yin, X.G. Wan, Tuning carrier mobility of phosphorene nanoribbons by edge passivation and strain, Phys. Lett. A 380 (2016) 614–620, http://dx.doi.org/10.1016/j.physleta.2015.11.019.

[28] Z. Nourbakhsh, R. Asgari, Excitons and optical spectra of phosphorene nanoribbons, Phys. Rev. B 94 (2016) 035437, http://dx.doi.org/10.1103/PhysRevB.94.035437.

[29] G. Yang, S. Xu, W. Zhang, T. Ma, C. Wu, Room-temperature magnetism on the zigzag edges of phosphorene nanoribbons, Phys. Rev. B 94 (7) (2016) 075106.
[30] F. Xie, Z.-Q. Fan, X.-J. Zhang, J.-P. Liu, H.-Y. Wang, K. Liu, J.-H. Yu, M.-Q. Long, Tuning of the electronic and transport properties of phosphorene nanoribbons by edge types and edge effects, Org. Electron. 42 (2017) 21–27, http://dx.doi.org/10.1016/j.orgel.2016.12.020.
[31] Z.-Q. Fan, W.-Y. Sun, S.-W. Jiang, J.-W. Luo, S.-S. Li, Two-dimensional Schottky contact structure based on in-plane zigzag phosphorene nanoribbon, Org. Electron. 44 (2017) 20–24, http://dx.doi.org/10.1016/j.orgel.2017.02.002.
[32] J. Xiao, M. Long, C.S. Deng, J. He, L.L. Cui, H. Xu, Electronic Structures and carrier mobilities of blue phosphorus nanoribbons and nanotubes: a first-principles study, J. Phys. Chem. C 120 (8) (2016) 4638–4646.
[33] T. Hu, J. Hong, Electronic structure and magnetic properties of zigzag blue phosphorene nanoribbons, J. Appl. Phys. 118 (2015) 054301, http://dx.doi.org/10.1063/1.4927848.
[34] R. Swaroop, P.K. Ahluwalia, K. Tankeshwar, A. Kumar, Ultra-narrow blue phosphorene nanoribbons for tunable optoelectronics, RSC Adv. 7 (2017) 2992–3003, http://dx.doi.org/10.1039/c6ra26253h.
[35] L. Kou, T. Frauenheim, C. Chen, Phosphorene as a superior gas sensor: selective adsorption and distinct I–V response, J. Phys. Chem. Lett. 5 (2014) 2675–2681.
[36] J. Dai, X.C. Zeng, Bilayer phosphorene: effect of stacking order on bandgap and its potential applications in thin-film solar cells, J. Phys. Chem. Lett. 5 (7) (2014) 1289–1293, http://dx.doi.org/10.1021/jz500409m.
[37] Q.S. Yao, C.X. Huang, Y.B. Yuan, Y.Z. Liu, S.M. Liu, K.M. Deng, E.J. Kan, Theoretical prediction of phosphorene and nanoribbons as fast-charging Li ion battery anode materials, J. Phys. Chem. C 119 (12) (2015) 6923–6928.
[38] D. Caklr, C. Sevik, F.M. Peeters, Significant effect of stacking on the electronic and optical properties of few-layer black phosphorus, Phys. Rev. B – Condens. Matter Mater. Phys. 92 (2015) 1–8.
[39] J.H. Lin, H. Zhang, X.L. Cheng, First-principle study on the optical response of phosphorene, Front. Phys. 10 (4) (2015) 1–9.
[40] J.M. Soler, E. Artacho, J.D. Gale, A. García, J. Junquera, P. Ordejón, D. Sánchez-Portal, The siesta method for ab initio order- n materials simulation, J. Phys.: Condens. Matter 14 (2002) 2745–2779.
[41] J.P. Perdew, K. Burke, M. Ernzerhof, Generalized gradient approximation made simple, Phys. Rev. Lett. 77 (18) (1996) 3865.
[42] C.G. da Rocha, P.A. Clayborne, P. Koskinen, H. Häkkinen, Optical and electronic properties of graphene nanoribbons upon adsorption of ligand-protected aluminum clusters, PCCP 16 (8) (2014) 3558–3565.
[43] Z. Zhang, W. Guo, Energy-gap modulation of BN ribbons by transverse electric fields: first-principles calculations, Phys. Rev. B 77 (7) (2008) 075403.